

# TRANSVERSE MULTI-PASS BEAM BREAKUP SIMULATION FOR KEK ERL LIGHT SOURCE

S.Chen\*, M.Shimada, N.Nakamura, D.Zhou, KEK, Oho 1-1, Tsukuba, 305-0801, Japan  
 K. Liu, S. Huang, IHIP, Peking University, Beijing 100871, China

## Abstract

In this paper, simulation results of the transverse multi-pass beam breakup for KEK ERL light source are presented.

## INTRODUCTION

An X-ray synchrotron light source based on a multi-GeV ERL is under design in KEK, which is expect to be a successor of the existing synchrotron light sources of Photon Factory in KEK [1]. A preliminary design report of this project has been published in 2012 [2,3]. An average beam current up to 100mA is required for KEK ERL light source. It is known that the multi-pass transverse beam breakup could be a possible limitation to the average current. It is primarily contributed by a positive feedback between the recirculated bunch with transverse offset and insufficiently damped dipole HOMs in superconducting cavity. If the average current is larger than a certain value which is called threshold current, exponential growth of HOM power and transverse oscillation amplitude will occur and thus cause beam breakup. A two-dimensional analytical formula for the multi-pass BBU threshold current is [4]

$$I_{th} = -\frac{2pc}{e\left(\frac{\omega}{c}\right)\left(\frac{R_d}{Q}\right)Q_{ext}M_{12}^*\sin(\omega T_r)}, \quad (1)$$

where  $(R_d/Q)$  is the shunt impedance of the dipole mode in the cavity,  $Q_{ext}$  is the external quality factor,  $\omega$  is the HOM frequency,  $T_r$  is the bunch recirculating time, and

$$M_{12}^* = T_{12} \cos^2 \theta + \frac{1}{2}(T_{14} + T_{23}) \sin 2\theta + T_{34} \sin^2 \theta,$$

where  $T_{ij}$  are the elements of the pass-to-pass transport matrix and  $\theta$  is the polarization angle of the dipole HOM.

Eq. 1 shows the main determinants of multi-pass BBU instability in an ERL. This formula only valids in the case of single cavity, single HOM and  $M_{12}^* \sin(\omega T_r) < 0$ . In real cases, the situation is more complicated. It's necessary to use simulation codes to compute the BBU threshold current. In this paper, the code *bi* [5] based on particle tracking is used to simulate the multi-pass BBU effect of KEK ERL light source. Some features of the BBU of high energy ERLs are then discussed based on the simulation results.

## KEK 3-GeV ERL LIGHT SOURCE

Several linac configurations have been designed for KEK ERL light source. In this paper, we are referring two of

\* chensi@post.kek.jp

them. One configuration consists of 28 cryomodules with 8 cavities in each cryomodule. The cavity gradient is about 13.4 MV/m and the full energy is about 3.01 GeV [2]. The other configuration consists of 34 cryomodules of the same structure. The cavity gradient is about 12.5 MV/m and the full energy is about 3.41 GeV [6].

To improve the dipole HOM damping, a 9-cell KEK-ERL mode-2 cavity (shown in Fig. 1) with a larger iris diameter compared with TESLA-type cavity and two large beam pipes to provide stronger HOM damping [7]. Several major dipole HOMs in the mode-2 cavity are listed in Table 1. A previous work shows the BBU threshold current of more than 600 mA can be achieved when applying this type of cavity to a 5-GeV ERL configuration [8].

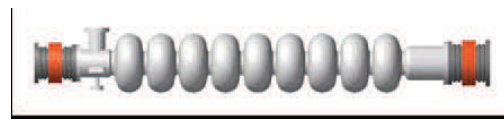


Figure 1: 1.3 GHz 9-cell KEK-ERL mode-2 cavity

Table 1: Major Dipole HOMs in KEK-ERL 9-cell Cavity

$f$ GHz	$Q_e$	$R/Q$ $\Omega/cm^2$	$(R/Q)Q_e/f$ $\Omega/cm^2/GHz$
1.835	$1.1010 \times 10^3$	8.087	4852
1.856	$1.6980 \times 10^3$	7.312	6691
2.428	$1.6890 \times 10^3$	6.801	4732
3.002	$2.9990 \times 10^4$	0.325	3246
4.011	$1.1410 \times 10^4$	3.210	9135
4.330	$6.0680 \times 10^5$	0.018	2522

## BBU SIMULATION RESULTS

### Lattice Configuration

The focusing effect of the RF field in the superconducting cavity is considered in the simulation. The Rosenzweig's form of the transport matrix for a pure  $\pi$ -mode standing-wave cavity [9] is applied in the simulation, i.e.,

$$M_{cav} = \begin{pmatrix} \cos \alpha - \sqrt{2} \sin \alpha & \sqrt{8} \frac{\gamma_i}{\gamma} \sin \alpha \\ -\frac{3}{\sqrt{8}} \frac{\gamma'}{\gamma_f} \sin \alpha & \frac{\gamma_i}{\gamma_f} [\cos \alpha + \sqrt{2} \sin \alpha] \end{pmatrix}, \quad (2)$$

where  $\alpha = \frac{1}{\sqrt{8}} \ln \frac{\gamma_f}{\gamma_i}$ ,  $\gamma_{i(f)}$  is the initial (final) relativistic factor of the particle,  $\gamma' = qE_0 \cos(\Delta\phi)/m_0c^2$  where  $E_0$  is the maximum particle energy gain from the RF cavity and  $\Delta\phi$  is the phase of acceleration.

## Betatron Phase Advance

As can be seen in Eq. 1, the BBU threshold current is a function of  $M_{12}^*$ . We assume that there is no x-y coupling in the recirculating loop and each dipole HOM has two different directions of polarizations ( $x$  ( $\theta = 0^\circ$ ) and  $y$  ( $\theta = 90^\circ$ )). Thus the value of  $T_{12}(T_{34})$  for the transport can be expressed with  $\beta$ -function and betatron phase advance as follows,

$$T_{12}(T_{34})(i \rightarrow f) = \sqrt{\frac{\beta_i \beta_f}{P_i P_f}} \sin \Delta\psi. \quad (3)$$

Eq.3 indicates that there is an dependency of BBU threshold current to the betatron phase advance. In ERL, the phase advance of the recirculating loop is usually flexible. Thus, we need to scanned the betatron phase advance from 0 to  $2\pi$  and simulated the BBU threshold current of both the two linac configuration. The results are shown in Fig.2.

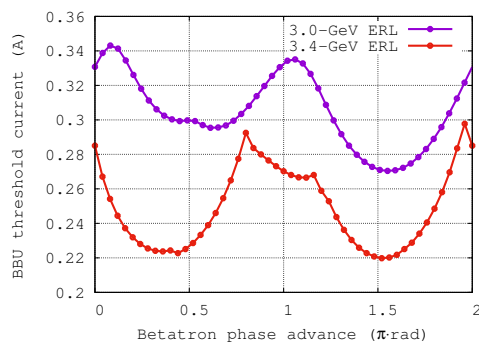


Figure 2: BBU threshold current of two existing design of lattice. Blue: 3.0-GeV ERL configuration. Red: 3.4-GeV ERL configuration

The maximum BBU threshold current is found to be about 342 mA for the 3.01-GeV configuration and 300 mA for the 3.41-GeV configuration. The minimum BBU threshold current is 270 mA for the 3.01-GeV configuration and 220 mA for the 3.41-GeV configuration. The BBU threshold currents of both configurations meet the requirement of 100 mA average current.

## HOM Frequency Randomization

In the previous simulation, we did not consider the possible HOM randomization due to the cavity shape inhomogeneous due to fabrication error. The simulation [10] shows that the randomization of both HOM frequency and external quality factor ( $Q_{ext}$ ) are naturally introduced during manufacturing more than one cavity. We assume the frequency randomization of the same type of HOM in different cavities in the linac to be a Gaussian distribution with desired rms frequency spread width  $\sigma_f$ . 1000 different sets of the HOM data with  $\sigma_f = 1$  MHz are generated in the linac cavities of the 3.0-GeV ERL scheme, and calculated the BBU threshold current of each set of HOM data. The statistical histogram of BBU threshold current distribution of this simulation is shown in Fig.3(a).

Due to the limited cavity number, the BBU threshold current with HOM frequency randomization shows an obvious statistical fluctuation. Therefore, usually the average BBU threshold current is employed to represent the BBU feature of such a condition. Fig. 3(b) shows the average BBU threshold current and its standard deviation of different frequency spread. It shows the average threshold can be significantly improved with the frequency spread  $\sigma_f$  increases, reaching about 940 mA when  $\sigma_f = 2$  MHz.

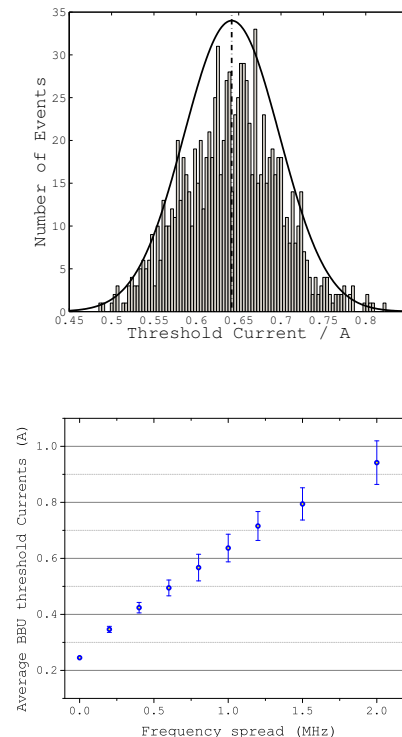


Figure 3: BBU threshold current with frequency randomization

## Quality Factor Randomization

Similar to the HOM frequency spread, the external quality factor of different cavities also shows a statistical distribution. We assume the distribution of  $Q_{ext}$  to be an uniform distribution from 0.1 to 10 times the nominal value listed in Table 1. A Gaussian frequency distribution of  $\sigma_f = 2$  MHz is applied as well. The BBU simulation is performed 100 times. The statistical distribution of the BBU threshold currents for the 3.01-GeV configuration is shown in Fig. 4.

## Return Loop Length

BBU threshold current is also a function of the recirculating loop length, which is represented in the form of  $T_r$ . Figure 5 shows the BBU threshold current versus the recirculating loop length variation in the form of  $\Delta T/T_0$ , where  $T_0$  is the time period of the accelerating base mode of the cavity.

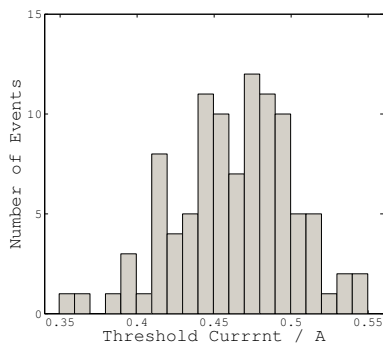


Figure 4: Statistical distribution of the BBU threshold current with  $Q_{ext}$  randomization.

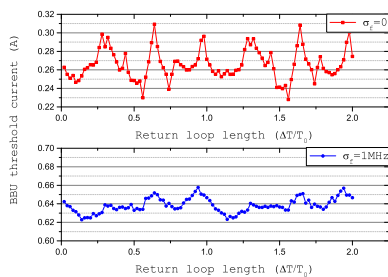


Figure 5: BBU threshold current vs. recirculating loop length.

In the case of  $\sigma_f = 0$ , the BBU threshold current shows a quasi-periodic oscillation, which is determined by the most threatening HOM in the KEK-ERL mode-2 cavity shown in Table. 1, i.e., the HOM with the frequency  $f = 4.011$  GHz. In the case of  $\sigma_f = 1$  MHz this oscillation is smeared because the coherent excitation of this HOM is disturbed by the frequency randomization.

## DISCUSSION

On the basis of the analysis above, we may roughly draw a conclusion that a BBU threshold current well above the designed average current can be obtained by applying KEK-ERL mode-2 cavity to KEK ERL light source. The HOM damping ability of the superconducting cavity plays an essential role in determining the BBU threshold current. A previous study gives a empirical criterion of the HOM properties to achieve 100 mA operation in an ERL [11]

$$(R/Q)Q_{ext}/f < 1.4 \times 10^5 (\Omega/cm^2/GHz),$$

As listed in Table1, all HOMs in KEK-ERL mode-2 cavity satisfy this criterion thus even the worst case of betatron phase advance shift still we can get sufficiently high threshold current.

It can be inferred from Eq. 1 that the cavities at low energy sections, i.e., the cavities at the start and the end of the linac, contribute more to the BBU. The BBU threshold current of each single cryomodule in the linac of the 3.41-GeV

configuration is calculated. The results are shown in Fig. 6. It is seen from Fig. 6 that threshold current of the first and last cryomodules are much smaller than the cryomodules in the middle of the linac.

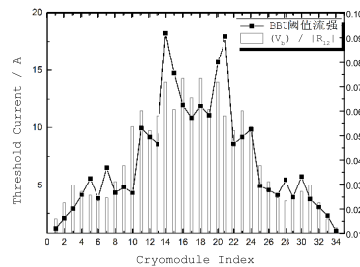


Figure 6: Cryomodule dependency of BBU threshold current.

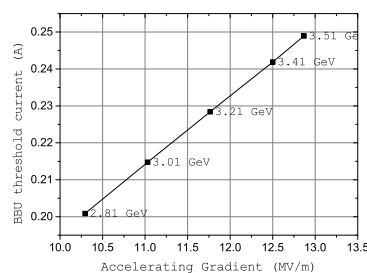


Figure 7: BBU threshold current vs. Cavity gradient.

We can also infer that an obvious approach to increase the BBU threshold current is to increase the accelerating gradient of the cavity. Figure 7 shows the BBU simulation of five ERL layouts with the same linac configuration but different accelerating gradient. A distinct increase of the BBU threshold current can be observed in the figure as the accelerating gradient increases. One can also expect a linear dependency of the BBU threshold current on the gradient of the cavity.

## REFERENCES

- [1] Nakamura N. in *Proceedings of IPAC2012, New Orleans, Louisiana, USA, 2012*:1040.
- [2] Energy Recovery Linac Preliminary Design Report. KEK, 2012.
- [3] Energy Recovery Linac Conceptual Design Report. KEK, 2012.
- [4] Pozdeyev E. *Phys.Rev.S.T-AB*, 8(5):054401, 2005.
- [5] *bi*, <http://www.lepp.cornell.edu/~ib38/bbu/>
- [6] Provided by Shimada M.
- [7] Sakai H., et al. in *Proc. of ERL07 Workshop*, pp:56–61.
- [8] Hajima R., Nagai R. light source. in *Proc. of ERL07 Workshop*, pp:133–138.
- [9] Rosenzweig G., Serafini L. *Phys. Rev. E*, 49(2):1599, 1994.
- [10] Xiao L., et al. in *Proc. of PAC07*, pp: 2454–2456.
- [11] Liepe M. in *Proc. of the 11th Workshop on RF Superconductivity*, pp: 115–119, 2003.

Content from this work may be used under the terms of the CC BY 3.0 licence (© 2015). Any distribution of this work must maintain attribution to the author(s), title of the work, publisher, and DOI.